Korean Journal of Chemical Engineering
https://doi.org/10.1007/s11814-024-00253-8

ORIGINAL ARTICLE

Recovery of Cobalt from Cathode of Lithium-Ion Battery Using Ternary Deep Eutectic Solvent

Xin Li[1] · Yin Li[1] · Qian Qiao[1] · Kun Wang[1] · Honghao Yu[1]

Received: 4 November 2023 / Revised: 14 July 2024 / Accepted: 5 August 2024

Abstract

A new ternary deep eutectic solvents, consisting of choline chloride, ethylene glycol, and benzoic acid, were designed for efficient leaching of valuable metals from lithium oxide of spent lithium-ion batteries. The influence of experiment parameters on the leaching of cobalt was systematically investigated and optimized by response surface methodology. The leaching kinetics were elucidated in detail. The leaching efficiency of cobalt reached almost 100%, when the temperature was 443.15 K, the time of 3 h, and the molar ratio of the choline chloride: ethylene glycol: benzoic acid of 1:1.6:0.4. The kinetics of Co leaching showed good agreement to the shrinking core model, in which the diffusion of solid product layers was the limiting step, and the apparent activation energy was about 77.22 kJ/mol. Infrared spectroscopy indicated that hydrogen donors provided multiple ligands to facilitate the solubilization of cobalt. The SEM analysis of the leachates showed that the edge of particles changed significantly, the particle size decreased, and the dissolution process appeared. The simultaneous realization of high efficiency green process is expected to bring the DES into practical application for recovery of cathode from spent lithium-ion batteries.

Keywords Cathode materials · Lithium-ion battery · Ternary deep eutectic solvent · Recovery

Introduction

Lithium-ion batteries (LIBs) play an important role in our highly electrified world, and the development of their related technologies will continue to lead to technological innovation in the field of energy storage. In recent years, the global demand for lithium batteries has continued to rise. In China, for example, LIBs production is 327 GWh in 2021, with a year-on-year growth rate of 130%, and it is estimated that in 2024, LIBs production exceeds 600 GWh, with a year-on-year growth rate of more than 80%. However, the short lifetime of LIBs means that a large number of spent LIBs will be generated in the future, it is estimated to generate 4 million tons of spent LIBs by 2040 [1]. Raising volumes of the LIBs production bring about considerable ecological risks and health hazards. Consequently, recycling of spent LIBs preserves the primary resources for the future by recovering valuable metals associated with it and keeps the environment clean [2–6]. For example, cobalt is a strategic material, which usually accounts for 15wt% of $LiCoO_2$ (LCO), a typical cathode material in commercial LIBs. It is regarded as an important supplement to natural sources of cobalt materials. Therefore, the recovery of valuable metals from spent LIBs is of great importance both in terms of environmental protection and primary resource conservation.

At present, the main technology for recycling spent LIBs includes pyrometallurgy and hydrometallurgy [7–10]. Pyrometallurgy, also known as incineration or dry metallurgy, uses a high-temperature furnace to reduce the component metal oxides of LIBs to an alloy. Among these, pyrometallurgy reigns supreme in industry despite the high energetic cost from the extreme temperatures (1400 °C or higher), and rampant off-gassing of harmful fumes, which require drastic safety precautions as well as the scrubbing of infrastructure to reduce subsequent pollution.

Hydrometallurgy is a method to selectively dissolve the cathode material in spent LIBs with suitable chemical reagents and to separate the metal elements in the leachate. Due to the high degree of comprehensive recovery of hydrometallurgy for valuable metals, the production process is easier to achieve continuity and automation; according to Sonoc

✉ Honghao Yu
honghaoyu@hotmail.com

[1] School of Materials Science and Engineering, Shenyang Ligong University, Shenyang 110159, China

Published online: 18 August 2024

[11], hydrometallurgy is one of the most viable options for recycling LIBs. Inorganic acid leaching is widely used due to its high efficiency and low cost.

A leaching system containing 2 mol/L H_2SO_4 and 15 vol% H_2O_2 was adopted by Sun et al. [12] and the leaching efficiencies of Li and Co reached 99% when reacted at 80 °C for 60 min [12]. However, the use of strong inorganic acids results in the release of Cl_2, SO_3, and NO_x, which poses a threat to the environment and human health and requires additional downstream processing to ensure proper management of these gases on an industrial scale [13]. In addition, the up-to-standard treatment of a large amount of acidic wastewater has become another major cost source for enterprises.

Recently, a green solvent named deep eutectic solvent (DES) may be an alternative to solve the above problems. In 2003, the concept of DES was first introduced by Abbott [14]. In the past 2 decades, DES have attracted much attention as solvents that are easy to prepare, low cost, environmentally friendly, and biodegradable [15–17]. In 2006, the solubility of 17 commonly available transition metal oxides in elemental mass series Ti through Zn was determined in three DES based on choline chloride (ChCl) by Abbott [18].

Landa-Castro et al. used three different compositions of DES as leaching media for recycling Co and Ni from spent Ni-MH batteries to synthesize Ni–Co alloys [19]. The solubility of DES to transition metal oxides brings new opportunities for green recycling of spent LIBs. In addition, DES could be reused after removing metal ions from leachate through extraction [20] or electrodeposition [21]. As a result, many researchers have devoted their attention to recycling spent LIBs via DES. ChCl is a commonly available feed additive, and is also used as hydrogen-bond acceptor (HBA) in the synthesis of DES. There are a few reports on the recovery of spent LIBs with ChCl-base DES [21–26]. Tran et al. [21] are among the first in leaching cobalt from high concentration Co-DES solution (10 mg LCO with 50 mg DES, ChCl + ethylene glycol (EG)) and the leaching efficiencies of Co and Li were both higher than 90%. However, the reaction temperature and time were still high to be 220 °C for 24 h, which is not beneficial to commercial operation. Wang et al. [22] dissolved 10 mg of LCO powder in 10 g ChCl + urea DES, more than 95% of the cobalt was leached from LCO-based materials. Pier Giorgio Schiavi et al. [25] used ChCl + EG DES for the selective recovery of cobalt from mixed LIBs, and the leaching efficiencies attained 90% for cobalt and only 10% for nickel. Using ChCl + formic acid DES, the leaching efficiency of Co was as high as 99.0% at 70 °C. However, many problems still need to be solved urgently in ChCl-based DES, in particular the leaching harsh reaction conditions and high viscosity of this kind of DES for hard liquid–solid separation. The selection and combination of hydrogen-bond donors are more important. Given that EG has a certain reduction ability and low viscosity [27] while benzoic acid has a strong coordination ability (carboxyl groups) and certain proton activity, they can serve as ideal solvent compositions of DESs [28].

To further solve the problems of low efficiency and subsequent treatment caused by high viscosity, for the first time, the leaching of the cathode materials LCO with ternary ChCl + EG + benzoic acid (BA) was systematically studied. Of particular, this work was devoted to finding the optimal operating conditions for the leaching efficiency of cobalt from LCO by the response surface methodology (RSM) method. Furthermore, the leaching of cobalt kinetics in ternary DES was investigated and the related mechanism was proposed.

Experimental

Materials and Reagents

Reagents include choline chloride ($C_5H_{14}ClNO$, A.R.), glycol ($C_2H_6O_2$, A.R.), and benzoic acid ($C_7H_6O_2$, A.R.). The materials of LCO were obtained by manual disassembly from a local battery recycling company. ChCl was purchased from American McLean Company with analytical grade, glycol was purchased from Tianjin Fuyu Fine Chemical Co. Ltd. with analytical grade, others were purchased from Tianjin Damao Chemical Reagent Factory with analytical grade, and all solutions were prepared using deionized water.

Synthesis of the Ternary DES

The molar ratio of ChCl to hydrogen donor was fixed at 1:2. EG and BA were combined as hydrogen donors, and their molar ratios varied between 0.9: 0.1 and 0.4:0.6, abbreviated to $M_{ChCl:EG:BA}$. The ChCl, EG, and BA were mixed in a sealed glass container, and heated in an oil bath at 323 K, stirring until clear and transparent homogeneous solution was formed [15].

Leaching of Cobalt from the Cathode Material by DESs

Figure 1 shows the schematic of the experimental procedure. For example, the as-prepared DES were heated to a specified temperature in an oil bath again, the cathode material was added with stirring. After reacted for a period of time, the sample was centrifuged to obtain the leachate and residue. The concentration of cobalt in the leachate was measured, and the leaching efficiency of cobalt was calculated by Eq. (1).

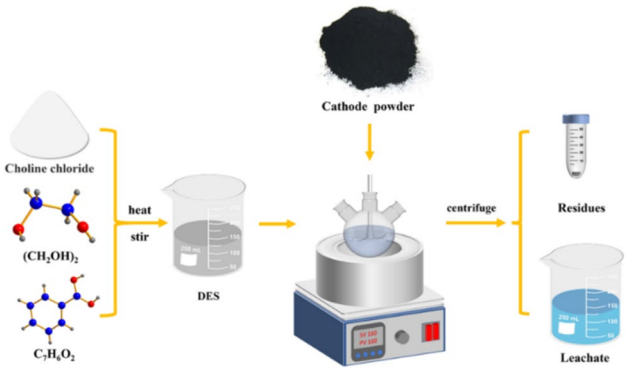

Fig. 1 Schematic of the experimental procedure

$$\eta = \frac{c \times v}{m} \times 100\% , \quad (1)$$

where c is the concentration of cobalt in the leachate, g/L; v is the volume of the leachate, L; and m is the quality of Co in the raw materials, g.

Analytical Methods

The morphological characterization was performed using scanning electron microscopy (SEM, S-3400N, HITACHI, Japan). The mineralogical analysis was performed using X-ray diffraction (XRD, Ultimaz V, Rigaku, Japan). The data were collected by step scanning with a scanning rate of 10°/min and a scanning angle (2θ) of 10°–90°. The chemical binding energy of cobalt in the residues was analyzed using X-ray photoelectron spectroscopy (XPS, ESCALAB 250Xi, Thermo Fisher, U.S.). The leachate was analyzed using Fourier transform infrared spectrometer (FT-IR, Nicolet iS50, Thermo Fisher).

Results and Discussion

Single Factor Experiments

The effects of reaction temperature, reaction time, molar ratio of benzoic acid, and stirring rate on the leaching efficiency of cobalt were investigated as shown in Fig. 2.

Under the conditions of $M_{ChCl:EG:BA} = 1:1.6:0.4$, the stirring rate of 500 r/min, and reaction time of 1 h, the effect of reaction temperatures on the leaching efficiency of cobalt was explored. From Fig. 2a, it can be seen that the leaching efficiency of cobalt increases obviously with the increasing temperature from 373.15 to 453.15 K. The leaching efficiency of cobalt reaches a peak of 99% at 453.15 K, and it does not change significantly during 453.15–473.15 K. The results show that the reaction temperature range required by the response surface analysis experimental design is 373.15–453.15 K. As the temperature increases, DES molecules gradually become active, and the opportunities for mutual contact with LCO greatly increase, which is also conducive to faster dissolution of valuable elements in LCO.

To examine the effect of time on cobalt leaching efficiency, time was varied in the range of 0.5–4 h. Other parameters maintained during the leaching include the following: the conditions of $M_{ChCl:EG:BA} = 1:1.9:0.1$, the stirring rate was 500 r/min, and the reaction temperature was 413.15 K. As can be seen from Fig. 2b, when the reaction time increases, the leaching efficiency of cobalt also increases. The leaching efficiency of cobalt increases 14.1% between 0.5 and 1.5 h, but it increases only 1.8% between 3 and 4 h. The results show that the reaction time selected by the response surface analysis experiment is between 1 and 3 h.

To test the effect of the molar ratio of benzoic acid on cobalt leaching efficiency, other experimental conditions are fixed at the temperature: 433.15 K, stirring rate: 500 r/min, and reaction time: 3 h. It can be seen in Fig. 2c that with the increase of the molar ratio of benzoic acid, the leaching efficiency of cobalt also increases, and the leaching efficiency reaches a peak of 99.9% after $M_{ChCl:EG:BA} = 1:1.5:0.5$. However, it increases smaller and smaller between 0.1 and 0.5 and does not change after 0.5. The results showed that the molar ratio of benzoic acid selected for the response surface analysis experiment is between 0.1 and 0.5. The acidity of the system mentioned in the literature is one of the factors determining the leaching efficiency of LCO[]. The selection and regulation of benzoic acid lie in providing corresponding acid value to improve the LCO leaching efficiency.

The effect of stirring rate (400–800 r/min) on the leaching efficiency of cobalt was examined in the conditions of $M_{ChCl:EG:BA} = 1:1.6:0.4$, reaction temperature of 433.15 K, and reaction time of 1 h. It can be seen from Fig. 2d, that with the increase in the stirring rate, the change in the leaching efficiency for cobalt is very small, and the leaching efficiency increases only 6% between 400 and 800 r/min. It hardly increases after 700 r/min. So subsequent experiments were conducted at 700 r/min. The results show that the stirring rate is not considered when performing the response surface analysis.

Response Surface Methodology Analysis

RSM is an optimization method combining experimental design and mathematical modeling, which is suitable for solving problems related to nonlinear data processing, and has been widely used in research fields such as machinery, chemical industry, and industrial process improvement [29].

Based on the single factor experiment, the response surface analysis method is used to optimize the process conditions of cobalt leaching in the cathode material of lithium

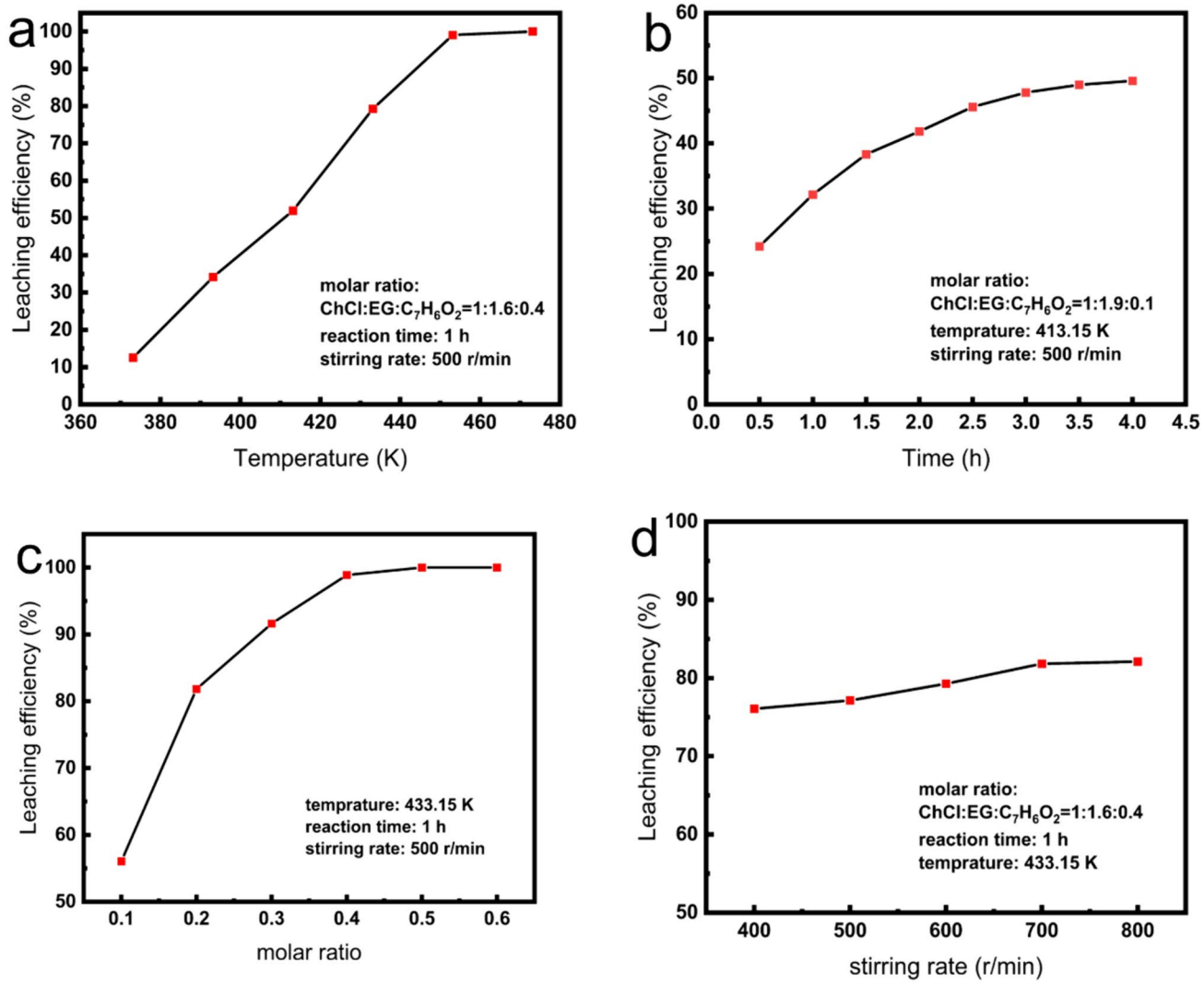

Fig. 2 Single factor experimental results: the effects on the leaching efficiency of cobalt: **a** reaction temperature, **b** reaction time, **c** molar ratio of benzoic acid, **d** stirring rate

Table 1 The experimental factor and level

Factors	Levels		
	− 1	0	+ 1
Time (h)	1	2	3
Temperature (K)	373.15	413.15	453.15
Molar ratio of benzoic acid	0.1	0.3	0.5

cobalt oxide batteries, and the leaching rate of cobalt is the response value. The experimental factor and level are seen in Table 1, and design and result are seen in Table 2.

According to Table 2, quadratic regression analysis was performed on the obtained data, as shown in Table 3.

The regression equation model used for the significance test showed a higher F value of 44.69, indicating that the model of the regression equation is significant. The signal-to-noise ratio (Adeq Precision) of the experiment was 23.2283, which was greater than 4, indicating that the designed experiment and the regression equation model obtained using the analysis are reasonable. Table 3 also lists the ANOVA of each influencing factor in the experiment. As can be seen from Table 3, the effects of A (temperature) and C (molar ratio of benzoic acid) on the leaching efficiency were highly significant ($P < 0.001$). The influence of three factors on leaching differed as reaction temperature (A) > molar ratio of benzoic acid (C) > time (B).

Figure 3 is the normal plot of residuals about leaching efficiency. The data points of 17 experimental samples were evenly and symmetrically distributed on the oblique line, which shows the good fit of the regression equation.

Table 2 The specific design and results

Run	Temperature (K)	Time (h)	Molar ratio of benzoic acid	Leaching efficiency (%)
1	413.15	1	0.5	63.64
2	413.15	3	0.5	83.679
3	373.15	2	0.1	3.694
4	413.15	2	0.3	63.099
5	373.15	2	0.5	23.621
6	373.15	3	0.3	15.316
7	413.15	2	0.3	61.567
8	453.15	3	0.3	99.99
9	413.15	2	0.3	68.897
10	453.15	2	0.1	65.767
11	373.15	1	0.3	6.076
12	413.15	3	0.1	47.785
13	453.15	1	0.3	92.678
14	413.15	2	0.3	60.785
15	413.15	2	0.3	59.458
16	453.15	2	0.5	99.99
17	413.15	1	0.1	32.15

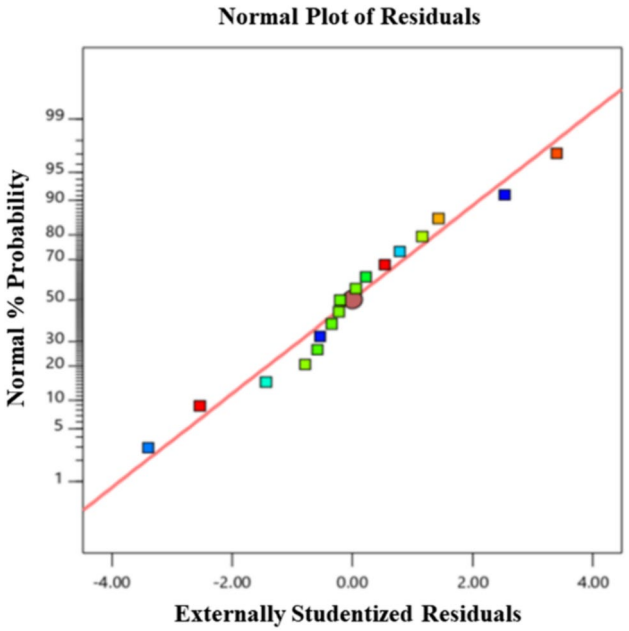

Fig. 3 The normal plot of residuals about leaching efficiency

Table 3 Quadratic regression analysis

Source	Sum of squares	*df*	Mean square	*F* value	*P* value
Model	14,728.98	9	1636.55	44.69	< 0.0001
A-time	11,990.65	1	11,990.65	327.41	< 0.0001
B-revolution	340.94	1	340.94	9.31	0.0186
C-rotation	1846.31	1	1846.31	50.41	0.0002
AB	0.9293	1	0.9293	0.0254	0.8779
AC	51.09	1	51.09	1.40	0.2761
BC	4.85	1	4.85	0.1324	0.7267
A^2	333.20	1	333.20	9.10	0.0195
B^2	0.5168	1	0.5168	0.0141	0.9088
C^2	131.92	1	131.92	3.60	0.0995
Residual	256.36	7	36.62		
Lack of fit	202.36	3	67.45	5.00	0.0771
Pure error	54.00	4	13.50		
Cor total	14,985.35	16			

Figure 4a shows that when the temperature is 413.15 K, the leaching efficiency increases less with the increase of time; and when the time is 3 h, the leaching efficiency increases greatly with the increase of temperature. It shows that temperature has a significant effect on the experiment, but time does not have a significant effect on the experiment. According to Fig. 4b, when the temperature is 413.15 K, the leaching efficiency increases with the increase of the molar ratio of benzoic acid; when the molar ratio of benzoic acid is 0.3, the leaching efficiency increases greatly with the increase of temperature. It shows that the molar ratio of benzoic acid and temperature have a significant effect on the experiment. According to Fig. 4c, when time is 2 h, the leaching efficiency increases with the increase of the molar ratio of benzoic acid; when the molar ratio of benzoic acid is 0.4, the leaching efficiency increases less with the increase of time. It shows that the molar ratio of benzoic acid has a significant effect on the experiment, but time has no significant effect on the experiment.

Finally, the Design-Expert software was used to optimize the experimental conditions and calculate the optimal conditions for leaching efficiency. The multivariate linear fitting of the response surface was used to generate the following equation:

$$Y = 62.76 + 38.71A + 6.53B + 15.19C - 0.482AB + 3.57AC + 1.1BC - 8.9A^2 - 0.3503B^2 - 5.6C^2. \quad (2)$$

The model-generated optimized reaction conditions were as follows: reaction temperature is 443.15 K, reaction time is 3 h, and $M_{ChCl:EG:BA}$ is 1:1.6:0.4. After three verification experiments, the average leaching efficiency was 99.95%, which was close to the theoretical prediction of 99.99%, indicating that the model can be used to predict the leaching efficiency. According to the response surface analysis, the temperature has a great influence on the leaching of cobalt, to explore the leaching mechanism of DES on cobalt, under the conditions of $M_{ChCl:EG:BA}$ is 1:1.6:0.4, the leaching kinetics analysis has been carried out.

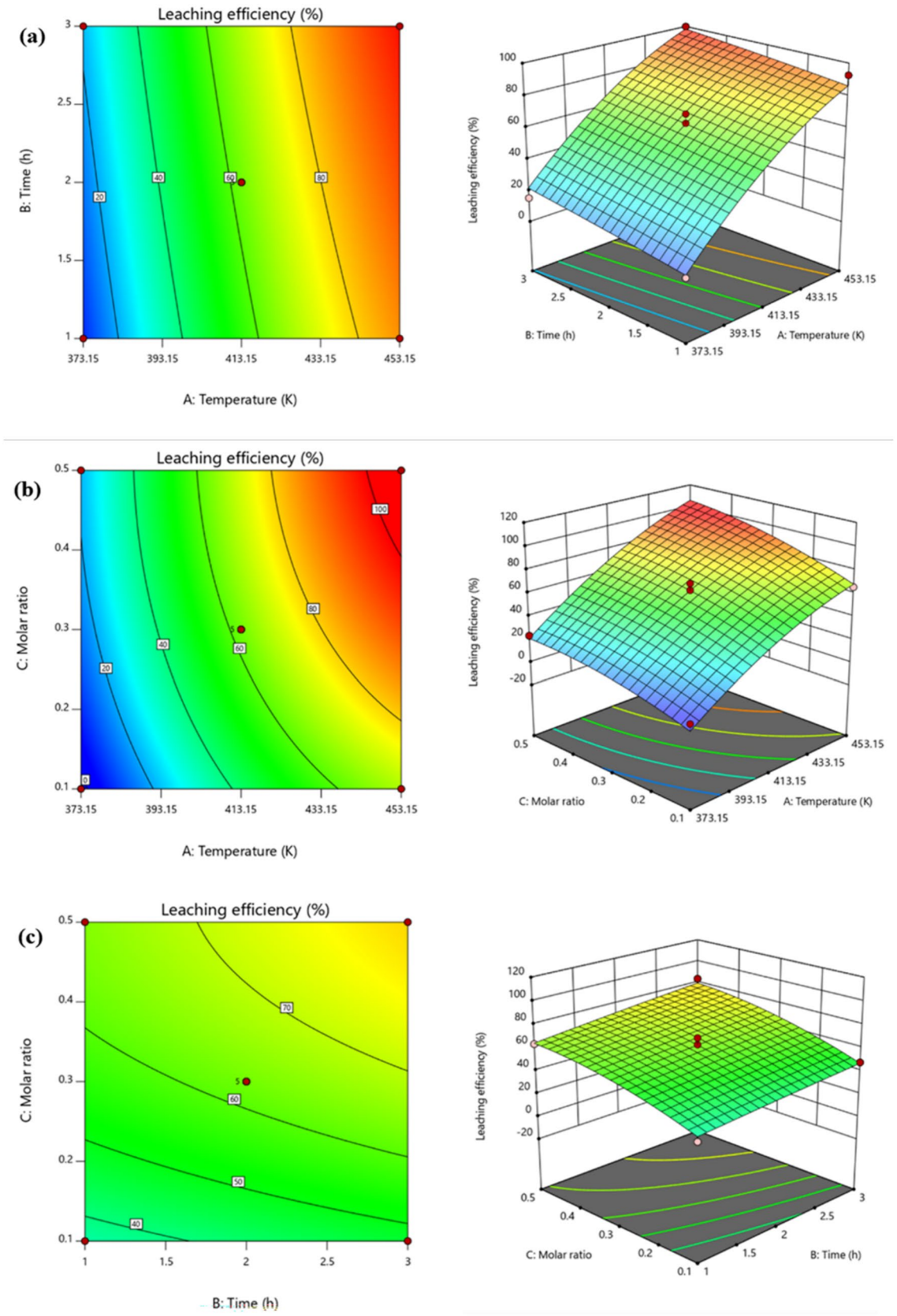

Fig. 4. 3D surface plot of the response surface analysis and the corresponding 2D contour plot: **a** temperature and time, **b** temperature and molar ratio of benzoic acid, **c** time and molar ratio of benzoic acid

Leaching Kinetics

The complexity of the reaction between the LCO and DES in the temperature range of 373.15–453.15 K is a typical liquid–solid reaction and requires a simplified model. The solid reactant is assumed to exist as round granules and to react from the outer surface toward the center of the particle without movement of the unreacted mass or the solid product. This can be called a shrinking unreacted-core model. According to the assumption, the reaction between LCO and DES is first order and the following three kinetic equations apply for different rate-controlling steps:

Chemical reaction control:

$$1-(1-\alpha)^{\frac{1}{3}}=\frac{k_r C_{A0}}{4\rho r_0}t=k_1 t. \tag{3}$$

Solid product layer diffusion control:

$$1-\frac{2}{3}\alpha-(1-\alpha)^{\frac{2}{3}}=\frac{D_s C_{A0}}{2\rho r_0^2}t=k_2 t. \tag{4}$$

The mixing control of the solid product layer diffusion and the interface chemical reaction:

$$\frac{\ln(1-\alpha)}{3}-1+(1-\alpha)^{-\frac{1}{3}}=k_3 t, \tag{5}$$

where α is the leaching efficiency of metal element, %; r_0 is the average radius of the cathode material particles, m; D_s is the mass transfer coefficient of the solid product layer diffusion, m s; k_r is the interface reaction rate constant; C_{A0} is the initial reactant concentration, kg/dm^3; ρ is the density of the cathode material, kg/m^3; t is the reaction time, min; k_1, k_2, and k_3 are interfaced chemical reaction, diffusion of the solid product layer diffusion, and the mixing control of the interface chemical reaction and the diffusion of the solid product layer diffusion, respectively, min^{-1}.

To reveal the control steps of LCO leaching in DES, the leaching rate conversion α at different temperatures is fitted to Eqs. (3), (4), and (5), as shown in Fig. 5b–d. The results show that Eq. (4) has a better linear trend at different temperatures (from 0 to 180 min). Plots of $1-\frac{2}{3}\alpha-(1-\alpha)^{\frac{2}{3}}$ vs. time show that leaching LCO at 373.15–453.15 K has a good correlation with kinetic Eq. (4) of the diffusion control of solid product layers. Therefore, leaching LCO in a ternary deep eutectic solvent (choline chloride-glycol-benzoic acid) is a solid product layer diffusion control process.

The apparent activation energy is calculated from the Arrhenius plots (Eq. 6) describing the relation of the natural logarithm of reaction rate constant (ln$K$) against the reciprocal of absolute temperature (1/T) as shown in Fig. 6.

$$\ln K=\ln A-\frac{E}{R}\cdot\frac{1}{T}, \tag{6}$$

where E is the apparent activation energy, A is the pre-exponential factor, and R is the molar gas constant.

The apparent activation energy is 77.219 kJ/mol, and the macroscopic dynamics equation leached by the LCO in DES can be described as:

$$1-\frac{2}{3}\alpha-(1-\alpha)^{\frac{2}{3}}=3.67\times10^6\exp\left(\frac{77219}{RT}\right)\cdot t. \tag{7}$$

To further confirm the formation of intermolecular hydrogen bonds between HBA and HBD, the FT-IR of pure components and as-prepared DESs is given in Fig. 7. From Fig. 7a, it can be found that nearly all the characteristic peaks of functional groups belonging to ChCl, EG, and BA still existed in the prepared DESs [30–34]. Here, the FT-IR spectra of EG, BA, and DESs were used to illustrate the shifting of characteristic peaks of the functional group after DES synthesis. The asymmetrical CCO stretching vibration band of ChCl occurred near 956 cm^{-1}. This meant that the Ch + group was not changed in the as-prepared DESs. The peak shape widened, and the peak position hardly changed (3296.3 cm^{-1}) for the O–H stretching vibration, which demonstrated that many intermolecular or tiny intramolecular hydrogen bonds were formed. The C–O, the stretching vibration characteristic peaks (EG), showed a blue shift (from 1078.0 and 1033.2 cm^{-1} separately at 1083.0 cm^{-1} and 1037.0 cm^{-1}). Besides, the stretching vibration characteristic peaks of –C=O in BA displayed a blue shift (from 1683.3 to1708.1 cm^{-1}). From Fig. 7b, it can be seen that the stretching vibration characteristic peaks of –C=O in as-prepared DESs displayed a slight blue shift (from 1078.0 to 1712.1 cm^{-1}). The higher energy implied a change in the electronic environment of –C=O. It may be accompanied by the generation of metal ions with oxygen coordination. DESs composed of HBD and ChCl (HBA), HBD as the oxygen atom acceptor, and the coordination of chloride ions and metal anions cause metal dissolution [32]. In the present system, whether there are multiple strong coordination environments to accelerate the dissolution of cobalt and the related dissolution mechanism need to be further investigated.

Characterization of the Residue

Upon the complement of the leaching experiments, the resulting residue is characterized. XRD patterns of the residue determined that the composition of the residue is still LCO, but the peak strength of the residue is significantly reduced, indicating that LCO is destroyed during leaching, as shown in Fig. 8a. XPS of the residue can show that the binding energy for cobalt in the residue is 778.6 eV, and indicate the valence state of cobalt in the residue is mainly

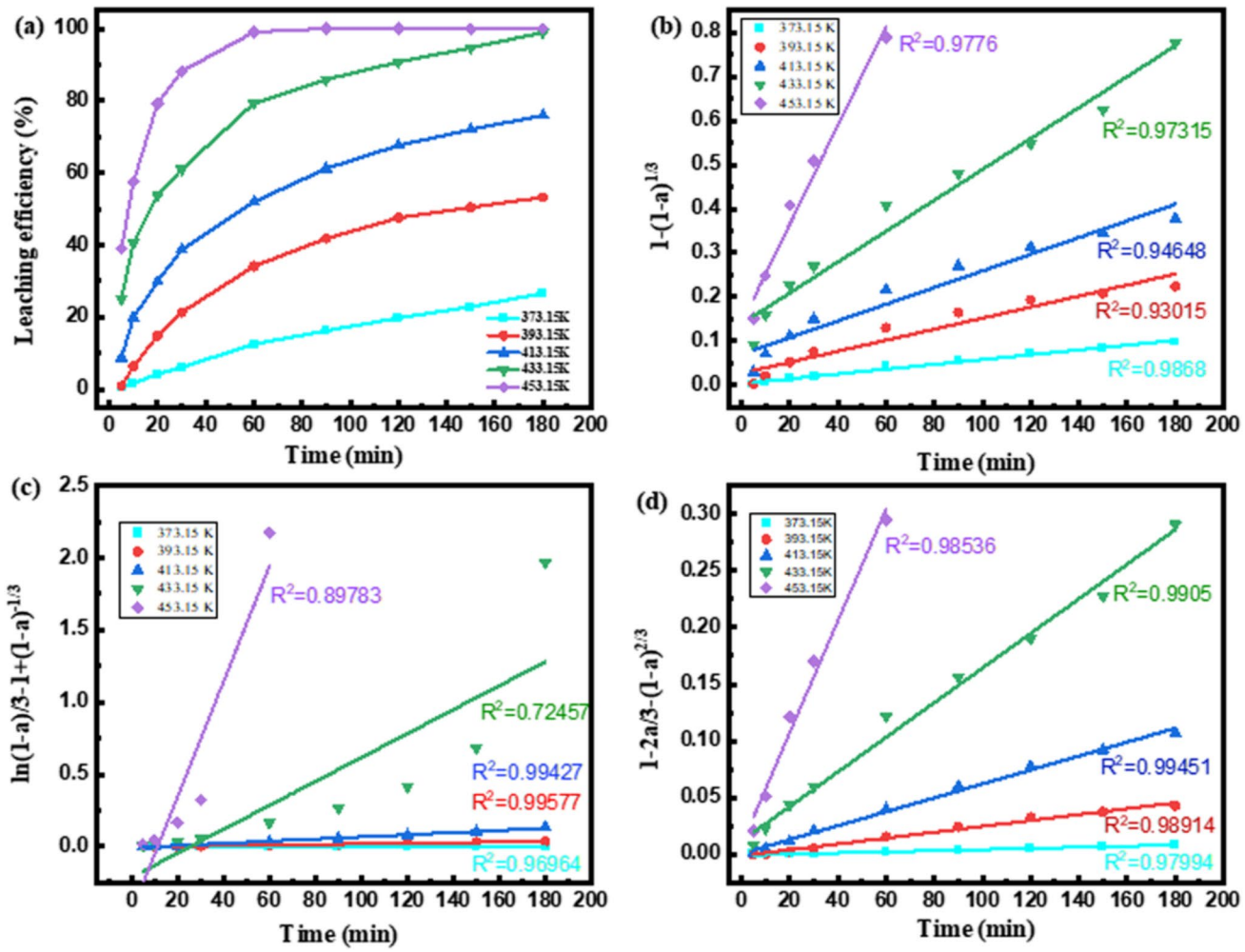

Fig. 5 Kinetic analysis of the choline chloride + glycol + benzoic acid leaching system. **a** Leaching efficiency at a different temperature, **b** plots of $1-(1-\alpha)^{\frac{1}{3}}$ vs. time based on **a**, **c** plots of $1-\frac{2}{3}\alpha-(1-\alpha)^{\frac{2}{3}}$ vs. time based on **a**, **d** plots of $\frac{\ln(1-\alpha)}{3}-1+(1-\alpha)^{-\frac{1}{3}}$ vs. time based on **a**

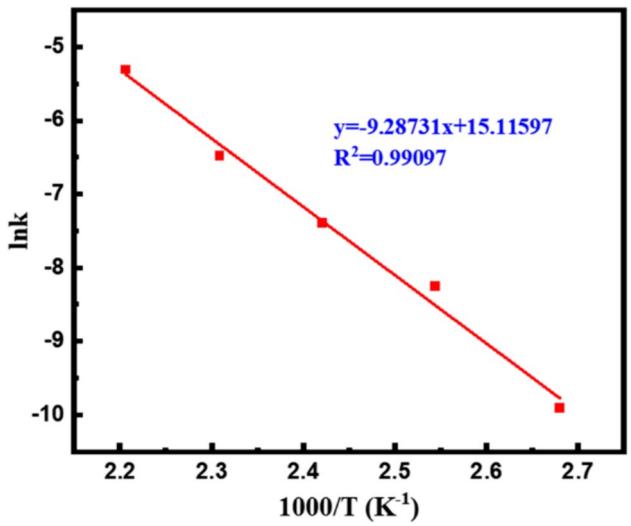

Fig. 6 Linearized Arrhenius plot to determine Ea of leaching of cobalt

Co^{3+}, as shown in Fig. 8b. SEM characterization of the residue, compared with the SEM characterization of the raw material shows that the surface of the raw material is smooth and the crystal form is intact, while the surface of the residue is eroded and the crystal form is destroyed, as shown in Fig. 9.

Conclusion

We designed and prepared a new deep eutectic solvent based on choline chloride, ethylene glycol, and benzoic acid to leach metals from lithium-ion batteries cathode material (LCO). The leaching efficiency of cobalt reached almost 100% when the temperature was 443.15 K, at the time of 3 h, and the molar ratio of the choline chloride:ethylene glycol:benzoic acid of 1:1.6:0.4.

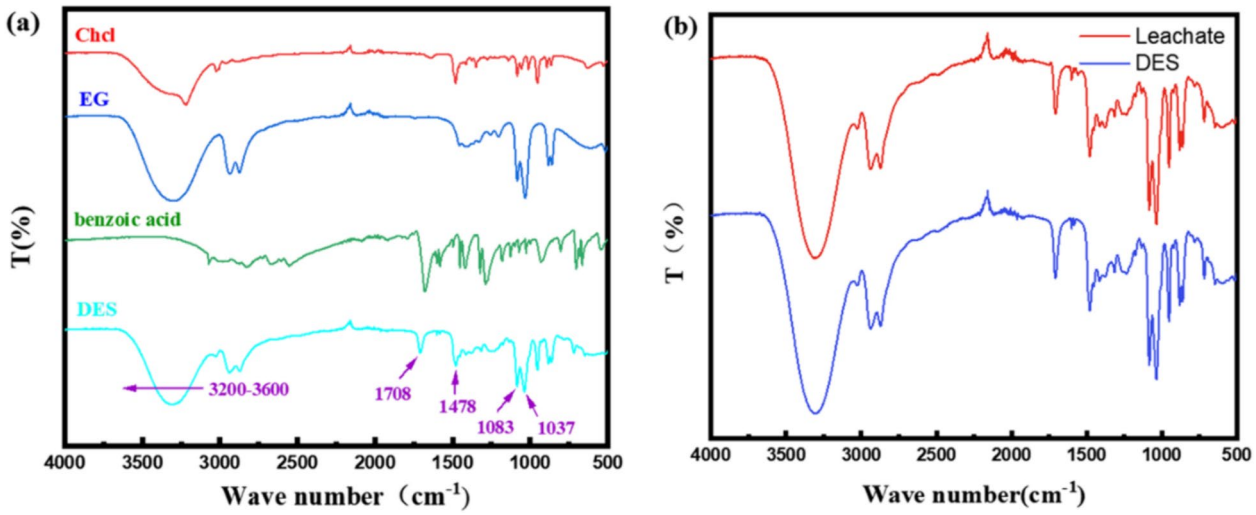

Fig. 7 **a** FT-IR spectra of choline chloride, glycol, benzoic acid, and DES (choline chloride:glycol:benzoic acid molar ratio of 1:1.6:0.4); **b** DES and leachate

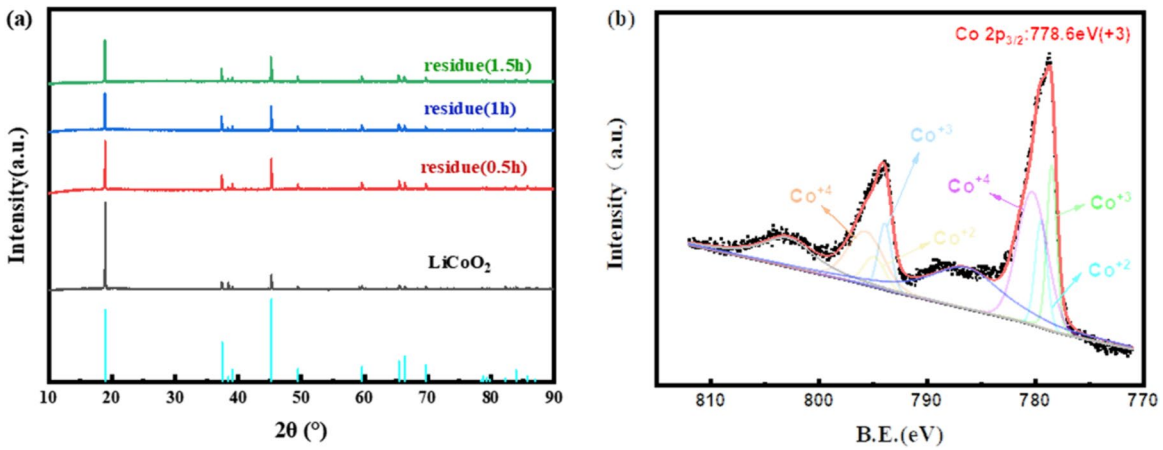

Fig. 8 **a** XRD of the cathode material and residues, **b** Gauss fitting of Co2p XPS spectra of the residues

Response surface methodology analysis can provide better optimization of cobalt leaching process parameters. The importance of each factor was experimentally quantified, and the order of their influence was reaction temperature > molar ratio of benzoic acid > time.

The kinetics of cobalt leaching showed good agreement to the shrinking core model, in which the diffusion of solid product layers was the limiting step, and the apparent activation energy was about 77.22 kJ/mol. Infrared spectroscopy indicated that hydrogen donors provided multiple ligands to facilitate the solubilization of cobalt. The SEM analysis of the leachates showed that the edge of particles changed significantly, the particle size decreased, and the dissolution process appeared. The simultaneous realization of high efficiency green process is expected to bring the DES into practical application for recovery of cathode from spent lithium-ion batteries.

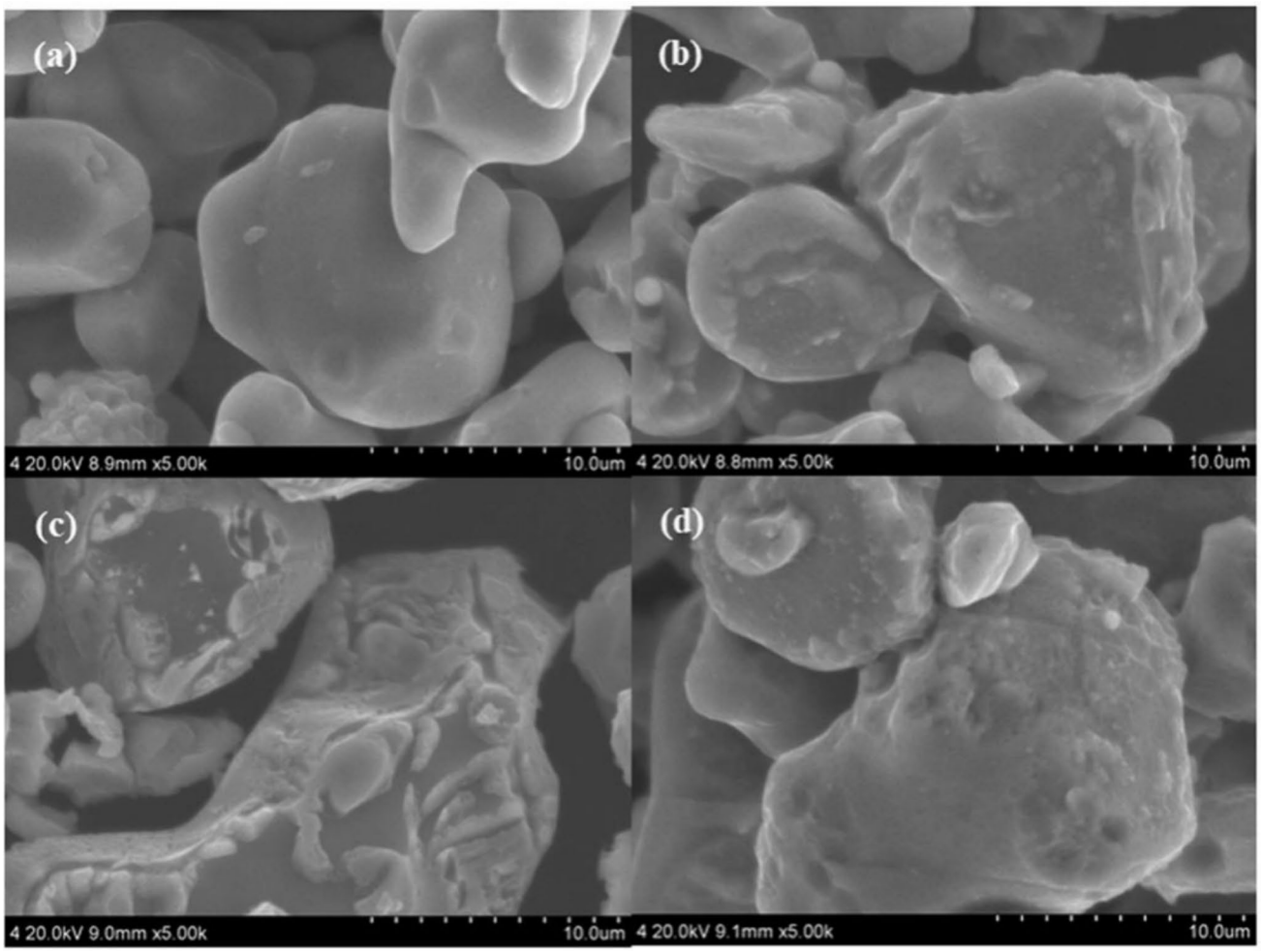

Fig. 9 **a** SEM of the cathode material, **d**–**f** SEM of the residues (leaching 0.5 h,1 h, and 1.5 h)

Acknowledgements The National Natural Science Foundation of China (No. U1360204 and No. 51304139), the Science and Technology Foundation of Liaoning Province, China (2023-MS-221) Basic Research Projects of the Educational Department of Liaoning Province (JYTMS20230215), China are acknowledged.

Data availability The data that support the findings of this study are available from the corresponding author upon reasonable request.

Declarations

Conflict of Interest The authors declare no competing financial interest.

References

1. W. Wang, Y. Zhang, X. Liu, S. Xu, A.C.S. Sustain, Chem. Eng. **7**, 12222 (2019)
2. X. Sun, H. Hao, F. Zhao, Z. Liu, Environ. Sci. Technol. **53**, 743 (2019)
3. S.P. Barik, G. Prabaharan, B. Kumar, Waste Manag. **51**, 222 (2016)
4. S. Chu, Y. Cui, N. Liu, Environ. Sci. Technol. **16**, 16 (2017)
5. J. Heelan, E. Gratz, Z. Zheng, Q. Wang, M. Chen, D. Apelian, Y. Wang, JOM **68**, 2632 (2016)
6. D. Larcher, J.-M. Tarascon, Nat. Chem. **7**, 19 (2015)
7. M. Assefi, S. Maroufi, Y. Yamauchi, V. Sahajwalla, Curr. Opin. Green Sustain. Chem. **24**, 26 (2020)
8. Y. Yao, M. Zhu, Z. Zhao, B. Tong, Y. Fan, Z. Hua, A.C.S. Sustain, Chem. Eng. **6**, 13611 (2018)
9. G. Harper, R. Sommerville, E. Kendrick, L. Driscoll, P. Slater, R. Stolkin, A. Walton, P. Christensen, O. Heidrich, S. Lambert, A. Abbott, K. Ryder, L. Gaines, P. Anderson, Nature **575**, 75 (2019)
10. X. Zheng, Z. Zhu, X. Lin, Y. Zhang, Y. He, H. Cao, Z. Sun, Engineering **4**, 361 (2018)
11. A. Sonoc, J. Jeswiet, V.K. Soo, Procedia CIRP **29**, 752 (2015)
12. L. Sun, K. Qiu, J. Hazard. Mater. **194**, 378 (2011)
13. Z.A. Kader, A. Marshall, J. Kennedy, Emerg. Mater. **4**, 725 (2021)
14. A.P. Abbott, G. Capper, D.L. Davies, R.K. Rasheed, V. Tambyrajah, Chem. Commun. **1**, 70 (2003)
15. V. Gotor-Fernández, C.E. Paul, J. Biotechnol. **293**, 24 (2019)
16. M. Shojaiepour, B. Aminshahidy, B. Dabir, Iran. J. Chem. Chem. Eng. **41**, 1095 (2022)
17. M. Piryaei, Iran. J. Chem. Chem. Eng. **41**, 135 (2022)
18. A.P. Abbott, G. Capper, D.L. Davies, K.J. McKenzie, S.U. Obi, J. Chem. Eng. Data **4**, 1280 (2006)

19. M. Landa-Castro, J. Aldana-González, M.G.M. Oca-Yemha, M. Romero-Romo, E.M. Arce-Estrada, M. Palomar-Pardavé, J. Alloys Compd. **830**, 154650 (2020)
20. N. Peeters, K. Binnemans, S. Riaño, Green Chem. **13**, 4210 (2020)
21. M.K. Tran, M.-T.F. Rodrigues, K. Kato, G. Babu, P.M. Ajayan, Nat. Energy **4**, 339 (2019)
22. H. Wang, M. Li, S. Garg, Y. Wu, M.N. Idros, R. Hocking, H. Duan, S. Gao, A.J. Yago, L. Zhuang, T.E. Rufford, Chemsuschem **14**, 2972 (2021)
23. F.-J. Albler, K. Bica, M.R.S. Foreman, S. Holgersson, M.S. Tyumentsev, J. Clean. Prod. **167**, 806 (2017)
24. S. Wang, Z. Zhang, Z. Lu, Z. Xu, Green Chem. **22**, 4473 (2020)
25. P.G. Schiavi, P. Altimari, M. Branchi, R. Zanoni, G. Simonetti, M.A. Navarra, F. Pagnanelli, Chem. Eng. J. **417**, 129249 (2021)
26. L. Chen, Y. Chao, X. Li, G. Zhou, Q. Lu, M. Hua, H. Li, X. Ni, P. Wu, W. Zhu, Green Chem. **23**, 2177 (2021)
27. W. Chen, J. Jiang, X. Lan, X. Zhao, H. Mou, T. Mu, Green Chem. **21**, 4748 (2019)
28. J.A. Dean, Mater. Manuf. Process. **4**, 687 (1990)
29. H. Lv, X. Chen, X. Zeng, Chaos Solitons Fractals **148**, 111048 (2021)
30. Y. Tian, W. Chen, B. Zhang, Y. Chen, R. Shi, S. Liu, Z. Zhang, T. Mu, Chemsuschem **15**, e202200524 (2022)
31. N. Peeters, K. Binnemans, S. Riaño, Green Chem. **22**, 4210 (2020)
32. J. Richter, M. Ruck, Molecules **25**, 78 (2020)
33. B. Li, Q. Li, Q. Wang, X. Yan, M. Shi, C. Wu, Phys. Chem. Chem. Phys. **32**, 19029 (2022)
34. C. Luo, Y. Zhang, X. Zeng, Y. Zeng, Y. Wang, J. Colloid Interface Sci. **288**, 444 (2005)